

Primordial Lithium and Big Bang Nucleosynthesis

S. G. Ryan*, T. C. Beers†, K. A. Olive‡, B. D. Fields§, J. E. Norris||

* *Physics Department, Open University, Walton Hall, Milton Keynes MK7 6AA, United Kingdom*

† *Department of Physics and Astronomy, Michigan State University, East Lansing, MI 48824, USA*

‡ *Theoretical Physics Institute, School of Physics and Astronomy, University of Minnesota, 116 Church Street, SE, Minneapolis, MN 55455, USA*

§ *Department of Astronomy, University of Illinois at Champaign-Urbana, 1002 West Green Street, Urbana, IL 61801, USA*

|| *Research School of Astronomy and Astrophysics, The Australian National University, Private Bag, Weston Creek Post Office, ACT 2611, Australia*

In the standard hot big bang nucleosynthesis (BBN) model^[1, 2], the primordial abundances of ^1H , ^2H , ^3He , ^4He , and ^7Li fix the baryon density of the universe, Ω_b , via the baryon-to-photon ratio, η , for a given Hubble parameter. Recent observations of Li show^[3] that its intrinsic dispersion in metal-poor stars is essentially zero, and the random error in the mean Li abundance is negligible. However, a decreasing trend in the Li abundance towards lower metallicity, plus ^6Li detections^[4, 5], indicate that its primordial abundance can be inferred only after allowing for nucleosynthesis processes in the Galaxy (Galactic chemical evolution, hereafter GCE). We show that the Li *vs* Fe trend provides a tough discriminant between alternative models for GCE of light-elements. We critically assess current systematic uncertainties, and determine the primordial Li abundance within new, much tighter limits. We show that the Li constraint on Ω_b is now limited principally by uncertainties in the nuclear cross-sections used in BBN *calculations*, not by the abundance itself. A clearer understanding of systematics allows for a much more accurate inference of the primordial Li abundance, sharpening the comparison with ^4He and deuterium and the resulting test of BBN. We find that the Li data are in good agreement with ^4He and with “high” deuterium values, but that low deuterium abundances are at best marginally within the Li range.

An important test of BBN is concordance between the observationally-inferred primordial abundances of the light elements. However, all current values involve considerable systematic uncertainties. Estimates of the ^4He primordial mass fraction, Y_p , had settled^[6] around $Y_p = 0.230 \pm 0.005$, but different systematics and underlying stellar He I absorption may imply a higher value^[7] near 0.245. For deuterium, quasar absorption line measurements give both “low”^[8, 9] abundances around $\text{D}/\text{H} = (3\text{--}5)\times 10^{-5}$ and “high”^[10, 11] values around $\text{D}/\text{H} = (15\text{--}25)\times 10^{-5}$. It is unclear which value (if either) represents the correct *primordial* value. ^3He presents even greater difficulties associated with its highly uncertain yield in low-mass stars^[12, 13], and currently provides unreliable constraints. Recent observations^[3] of Li have greatly improved, therefore we examine the random and systematic uncertainties associated with the primordial abundance and its interpretation with respect to BBN.

In inferring the primordial ^7Li abundance, $A(\text{Li})_p$ (where $A(\text{Li}) \equiv \log_{10}(n(\text{Li})/n(\text{H})) + 12.00$), from observations of metal-poor stars, systematic errors arise in: (1) the assessment of Li GCE prior to a given star forming; (2) the correction for depletion of a star’s initial surface Li; (3) the measurement of the current abundances; and (4) possible confusion by

anomalous objects. We examine each factor below, and summarise its impact in Table 1.

GCE: The GCE contribution to ${}^7\text{Li}$ was long believed to be negligible for metal-poor stars. However, observations of very metal-poor stars showing (1) lower Li abundances^[3] and (2) measurable ${}^6\text{Li}$ ^[4, 5] (which comes solely from Galactic cosmic ray (GCR) reactions), show that GCE cannot be ignored. Li GCE can be constrained either empirically from the observed evolution, or by modeling the sources and sinks of the element. Here we pursue both routes, partly to investigate the range of possible values, and partly to learn about GCE itself, since an accurate Li trend can constrain not only standard GCR and ν -process nucleosynthesis, but also other mechanisms which may produce Li in Population II, e.g., those suggested to produce primary beryllium along with Li. Sources of lithium in the oldest (Population II) stars are GCR nucleosynthesis of ${}^6\text{Li}$ and ${}^7\text{Li}$, and the supernova ν -process which produces ${}^7\text{Li}$ and ${}^{11}\text{B}$. The sink is astration — the destruction of Li in stellar interiors subsequently ejected into the interstellar medium (ISM).

Previously^[3] we examined GCE empirically, tracing the production of Li as the iron abundance increased, as a regression in logarithmic abundances:

$$A(\text{Li}) = \alpha + \beta[\text{Fe}/\text{H}] \quad (1)$$

where $[\text{Fe}/\text{H}] \equiv \log_{10}(\text{Fe}/\text{H})_{\text{star}} - \log_{10}(\text{Fe}/\text{H})_{\text{sun}}$. (Iron is a convenient and widely-measured diagnostic of GCE. It is always produced and never destroyed by stars, and thus serves as a chronometer.) We obtained values in the range $\beta = 0.07\text{--}0.16$, depending on the adopted $[\text{Fe}/\text{H}]$ values, the errors, and whether some points are excluded from the fit.

In the present work, we also investigate a fitting form which better follows Li production by GCE, and which simplifies the extrapolation to the primordial value. Li production is proportional to the cumulative number, N_{SN} , of Type II supernovae, as these are both GCR accelerators and the site of the ν -process. It thus is important to establish the primary tracer of such supernovae. If the cumulative supernova rate is well reflected by the iron abundance ($N_{SN} \propto \text{Fe}$), then a fit to *linear* abundance scales is appropriate:

$$\text{Li}/\text{H} = a' + b'\text{Fe}/\text{Fe}_{\odot} \quad (2)$$

Here a' directly measures the primordial ${}^7\text{Li}$ abundance (in the absence of systematic errors), while b' probes GCE. The linear fit parameters are sensitive to systematic Li errors; a change by Δ_{cal} dex in the log shifts both a' and b' by a factor $10^{\Delta_{\text{cal}}}$. We find $a' = 1.0\text{--}1.2 \times 10^{-10}$ and $b' = 40\text{--}180 \times 10^{-10}$.

On the other hand, if oxygen (which is more difficult to measure than iron) is a better tracer of Type II supernovae than iron, then $N_{SN} \propto O$, and we expect:

$$\text{Li}/\text{H} = a + b \text{O}/\text{O}_\odot \quad (3)$$

where $\text{O}/\text{O}_\odot = (\text{Fe}/\text{Fe}_\odot)^{1+\omega}$. Recent observations^[15, 16] show $\omega = -0.31$. In this case the data indicate $a = 0.9\text{--}1.2 \times 10^{-10}$ and $b = 9\text{--}34 \times 10^{-10}$.

We also compute the Li-Fe trend expected from a one-zone (closed box) GCE model^[17, 18, 19] which includes GCR and stellar nucleosynthesis, to compare with the observational results. (See Figure 1 caption for details.) Figure 1 shows the different Li components for the model with ${}^7\text{Li}_p = 1.23 \times 10^{-10}$. We fit the *model* by regressions of the forms (1) – (3), over the metallicity range of the recent data^[3], and find $b = 8.6 \times 10^{-10}$, $b' = 4 \times 10^{-9}$, and $\beta = 0.03 - 0.07$ (for input ${}^7\text{Li}_p = (0.9\text{--}1.9) \times 10^{-10}$). (The model’s “linear slopes”, b and b' , are independent of the input ${}^7\text{Li}_p$, while its “log slope”, β , does depend on ${}^7\text{Li}_p$.) This model’s Li GCE slopes (b , b' and β) are at the lower range of those found for the data, and for a closed-box model with only GCR and the ν -process. The poor agreement can be alleviated somewhat by manipulation of free parameters. For example, models including outflow of supernova ejecta (open box) and/or the inclusion of Li yields from AGB stars with $M < 5M_\odot$ produced steeper slopes, $b = (11 - 17) \times 10^{-10}$, $b' = (6 - 9) \times 10^{-9}$, and $\beta = 0.06 - 0.08$ (for various types of models with ${}^7\text{Li}_p = 1.23 \times 10^{-10}$), closer to the range seen in the data. This demonstrates the power of a reliable observational Li *versus* Fe trend to constrain the form and parameters of GCE models.

While comparison of model slopes with the observations can teach much about GCE, to infer the primordial Li we use the observed slopes (a procedure very similar to that used for ${}^4\text{He}$). From the linear fits to the data and our previous analysis^[3], we estimate that the GCE contribution to this metal-poor turnoff sample is $-0.11_{-0.09}^{+0.07}$ in the log (see Table 1).

Stellar Depletion: Stars burn Li, preserving at most a thin outer shell containing a few percent of the star’s mass. Possible *in situ* depletion of Li has long been regarded the major systematic uncertainty in inferring $A(\text{Li})_p$ from present-day abundances. Stellar evolution models predict the depletion factors. The simplest models imply almost no destruction (<0.05 dex, possibly $\lesssim 0.01$ dex) in very metal-poor turnoff stars^[21]. Models incorporating rotationally-induced mixing had predicted large depletion factors ~ 1 dex, though more recent efforts give lower values^[22] $\sim 0.2\text{--}0.4$ dex, and predict a range of depletion factors from star to star. The negligible intrinsic spread found for very metal-poor turnoff stars, $\sigma_{\text{int}} < 0.02$ dex, rules out rotational depletion even as low as 0.1 dex^[3]. As diffusion is also

absent^[23], we conclude that *in situ* depletion is minor, <0.1 dex, and possibly as little as ~ 0.01 dex.

Abundance Analyses: A Li abundance is derived via a parameter- and model-dependent analysis of a stellar spectrum, and systematic uncertainties propagate through to $A(\text{Li})_p$. Effective-temperature calibrations can differ by up to 150–200 K, higher temperatures resulting in higher Li abundances by 0.065 dex per 100 K. The scale initially adopted^[3] gives temperatures cooler than a more recent calibration^[24] by on average 120 K. We now adjust the abundances (Table 1) to the newer calibration^[24], but note that systematic errors of ± 120 K may still exist. This is one of the largest contributions to the uncertainty in $A(\text{Li})_p$. Fortunately, errors in the surface gravity, microturbulence, or damping parameters are negligible^[3]. Concerns about 1-D, plane-parallel model atmospheres have been reduced by simulations of solar-type granulation^[25] which show that the Li abundance is underestimated in the 1-D approximation by < 0.10 dex, and possibly < 0.01 dex, depending on the theoretical prescription for microturbulence. Consistent results in the metal-poor star HD 140283^[26] from the Li 6104 Å and 6707 Å lines inspire further confidence. However, models with greater convective flux can lead to Li abundances higher by 0.08 dex^[23]. Corrections for non-LTE^[27] are only -0.01 to -0.03 dex, and the uncertainty in the *gf*-values is only 0.02 dex (1σ)^[28].

Anomalous objects: Apart from the grossly Li-depleted star G186-26, only one of the remaining 22 objects in our sample was rejected by outlier-detection algorithms, changing the mean abundance by only ~ 0.005 dex. Similar un-recognised objects would affect the result by $\lesssim 0.01$ dex.

We can use the primordial element abundances to fix the one free parameter of the standard hot Big Bang nucleosynthesis (BBN) model^[1, 2], the baryon-to-photon ratio, η . From this, the baryon density of universe, Ω_b , may be deduced (for a given Hubble parameter, h). The inferred primordial abundance for Li (Table 1) is $A(\text{Li})_p = 2.09_{-0.13}^{+0.19}$ ($\text{Li}/\text{H} = 1.23_{-0.32}^{+0.68} \times 10^{-10}$), where the errors incorporate statistical (negligible) and systematic (more significant) effects. These errors are now sufficiently small that the range of corresponding η values (see below) is dominated by the uncertainties in the input nuclear cross-sections used BBN *calculations* rather than in the abundance. (Uncertainties in BBN give rise to a range of η values similar to those quoted below even for a perfectly determined value of $A(\text{Li})_p$.)

An important test of the BBN model is whether the inferred primordial abundances give concordant values of η . This is best tested by establishing likelihood distributions (as a func-

tion of η) for each element, convolving the theoretical and observational uncertainties^[2, 14]. Figure 2 shows the likelihood distributions for ${}^4\text{He}$ and four possible values of the primordial ${}^7\text{Li}$ abundance, all of which give excellent agreement. Overall concordance (at 95% CL) occurs for $\eta_{10} \equiv 10^{10}\eta = (1.4\text{--}4.9)$, $(1.5\text{--}4.4)$, $(1.7\text{--}3.9)$, and $(1.8\text{--}3.6)$, for $10^{10} \times {}^7\text{Li}/\text{H} = 1.9$, 1.6, 1.23, and 0.9 respectively. We can then use this result to assess the diverse deuterium values. For high D/H (2.0×10^{-4}), the peak of the D/H likelihood function (not shown) is at $\eta_{10} = 1.7$, (95% CL = 1.4–3.8), in very good agreement with the results from ${}^4\text{He}$ and ${}^7\text{Li}$. For low D/H (3.4×10^{-5}), the peak of the D/H likelihood function is at $\eta_{10} = 5.2$ (95% CL = 4.6–6.1), which would require ${}^7\text{Li}_p$ at the upper end of the possible range. However, if the low D/H was even only slightly higher, at 5×10^{-5} ^[29], then the D/H peak occurs at $\eta_{10} = 4.0$ (95% CL = 3.6–4.6), consistent with the ranges for ${}^4\text{He}$ and ${}^7\text{Li}$.

The baryon density corresponding to $\eta = (1.7\text{--}3.9) \times 10^{-10}$ is $\Omega_b = (0.025\text{--}0.057)/h_{50}^2$ (where h_{50} is the Hubble constant in units of $50 \text{ km s}^{-1} \text{ Mpc}^{-1}$), significantly below the lower 95% CL on $\Omega_m = 0.25^{+0.18}_{-0.12}$ ^[30], thus maintaining the requirement for non-baryonic dark matter.

Acknowledgements. The authors gratefully acknowledge discussions with Drs C. P. Deliyannis, M. Pinsonneault, and J. A. Thorburn on issues of stellar depletion. S.G.R. thanks the Institute of Astronomy of the University of Cambridge for provision of facilities following the closure of the Royal Greenwich Observatory. The work of KAO was supported in part by the Department of Energy at the University of Minnesota.

Correspondence should be addressed to S.G.R. (e-mail: s.g.ryan@open.ac.uk)

References

- [1] Schramm, D. N., & Turner, M. S. Big-bang nucleosynthesis enters the precision era. *Rev.Mod.Phys.* **70**, 303-318 (1998).
- [2] Fields, B. D., Kainulainen, K., Olive, K. A., & Thomas, D., Model independent predictions of big bang nucleosynthesis from ^4He and ^7Li : consistency and implications *New Ast.* **1**, 77-96 (1996).
- [3] Ryan, S. G., Norris, J. E., & Beers, T. C. The lithium Spite plateau: ultra-thin but post-primordial. *Astrophys.J.* in press, astro-ph/9903059 (1999).
- [4] Smith, V. V., Lambert, D. L., & Nissen, P. E. Isotopic Lithium abundances in nine halo stars. *Astrophys.J* **506**, 405-423 (1998).
- [5] Cayrel, R., Spite, M., Spite, F., Vangioni-Flam, E., & Cassé, M. New high S/N observations of $^6\text{Li}/^7\text{Li}$ blend in HD 84937 and two other metal-poor stars. *Astron.Astrophys.* **343**, 923-932 (1999).
- [6] Pagel, B. E. J., Simonson, E. A., Terlevich, R. J., & Edmunds, M. G. The primordial helium abundance from observations of extragalactic H II regions *Mon.Not.R.Astron.Soc.* **255**, 325-345 (1992).
- [7] Izotov, Y. I., & Thuan, T. X. The primordial abundance of ^4He revisited. *Astrophys.J.* **500**, 188-216 (1998).
- [8] Burles, S. & Tytler, D. The deuterium abundance towards QSO 1937-1009. *Astrophys.J.* **499**, 699-712 (1998).
- [9] Burles, S. & Tytler, D. The deuterium abundance towards QSO 1009+2956. *Astrophys.J.* **507**, 732-744 (1998).
- [10] Songaila, A., Cowie, L. L., Hogan, C. J., & Rugers, M. Deuterium abundance and background radiation temperature in high-redshift primordial clouds. *Nature* **368**, 599-604 (1994).
- [11] Carswell, R. F., Rauch, M., Weymann, R. J., Cooke, A. J., & Webb, J. K. Is there deuterium in the $z=2.32$ complex in the spectrum of 0014+813? *Mon.Not.R. Astron.Soc.* **268**, L1-4 (1994).

- [12] Galli, D., Palla, F., Ferrini, F., & Penco, U. Galactic evolution of D and ^3He . *Astrophys.J* **443**, 536-550 (1995).
- [13] Olive, K. A., Rood, R. T., Schramm, D. N., Truran, J. W., & Vangioni-Flam, E. What's the Problem with ^3He ? *Astrophys.J.* **444**, 680-685 (1995).
- [14] Fields B. D., & Olive, K. A. Model-independent predictions of big bang nucleosynthesis. *Phys. Lett.* **B368**, 103-111 (1996).
- [15] Israelian G., García-López, R. J., & Rebolo, R. Oxygen Abundances in Unevolved Metal-poor Stars from Near-Ultraviolet OH Lines. *Astrophys.J.* **507**, 805-817 (1998).
- [16] Boesgaard, A. M., King, J. R., Deliyannis, C. P., & Vogt, S. S. Oxygen in unevolved metal-poor stars from Keck ultraviolet HIRES spectra. *Astron.J.* **117**, 492-507 (1999).
- [17] Fields, B.D., & Olive, K.A., On the Evolution of Helium in Blue Compact Galaxies. *Astrophys.J.* **506**, 177-190 (1998).
- [18] Fields, B. D., & Olive, K. A. The revival of Galactic cosmic ray nucleosynthesis? *Astrophys.J.* **516**, in press (1999) astro-ph/9809277.
- [19] Fields, B. D., & Olive, K. A., The evolution of ^6Li in standard cosmic-ray nucleosynthesis. *New Astronomy* in press (1999) astro-ph/9811183.
- [20] Lambert, D. L., Heath, J. E., and Edvardsson, B. Lithium abundances for 81 F dwarfs. *Mon.Not.R.Astron.Soc.* **253**, 610-618 (1991).
- [21] Deliyannis, C. P., Demarque, P., & Kawaler, S. D. Lithium in halo stars from standard stellar evolution. *Astrophys.J.Suppl.* **73**, 21-65 (1990).
- [22] Pinsonneault, M. H., Walker, T. P., Steigman, G., & Narayanan, V. K. Halo Star Lithium Depletion. *preprint (astro-ph/9803073)* (1998).
- [23] Ryan, S. G., Beers, T. C., Deliyannis, C. P., & Thorburn, J. A. Lithium processing in halo dwarfs, and T_{eff} , [Fe/H] correlations on the Spite plateau. *Astrophys.J.* **458**, 543-560 (1996).
- [24] Alonso, A., Arribas, S., & Martinez-Roger, C. Determination of effective temperatures for an extended sample of dwarfs and subdwarfs (F0-K5). *Astron.Astrophys.Suppl.* **117**, 227-254 (1996).

- [25] Uitenbroek, H. The effect of photospheric granulation on the determination of the lithium abundance in solar-type stars. *Astrophys.J.* **498**, 427-440 (1998).
- [26] Bonifacio, P. & Molaro, P. Detection of the Li I λ 6104 transition in the Population II star HD 140283. *Astrophys.J.* **500**, L175-L177 (1998).
- [27] Carlsson, M., Rutten, R. J., Bruls, J. H. M. J., & Shchukina, N. G. The non-LTE formation of Li I lines in cool stars. *Astron.Astrophys.* **288**, 860-883 (1994).
- [28] Thorburn, J. A. The primordial Lithium abundance from extreme subdwarfs: New observations. *Astrophys.J.* **421**, 318-343 (1994).
- [29] Levshakov, S. A., Tytler, D., & Burles, S. Deuterium to hydrogen towards QSO 1009+2956 from a mesoturbulent model. *Astron.J.* submitted (1998) astro-ph/9812114.
- [30] Efstathiou, G., Bridle, S. L., Lasenby, A. N., Hobson, M. P., & Ellis, R. S. Constraints on Ω_Λ and Ω_m from distant Type Ia supernovae and cosmic microwave background anisotropies. *Mon.Not.R.Astron.Soc.* **303**, L47-L52 (1999).

Table 1 Inferred Primordial Lithium Abundance			
-			-
Observed: ^[3]	$\langle A(\text{Li}) \rangle_{-2.8} =$	+2.12	± 0.02
-			-
Corrections to apply (logarithmic):			(Estimated
(1) GCE/GCR:			Uncertainty)
previous analyses ^[3]	-0.14 to -0.05		
log data fit (eq. (1))	-0.20 to -0.09		
linear data fit (eq. (2))	-0.12 to -0.04		
linear data fit (eq. (3))	-0.16 to -0.05		
model fits (eq. (2)–(3))	-0.12 to -0.02		
Adopted (excludes model):		-0.11	$\begin{smallmatrix} +0.07 \\ -0.09 \end{smallmatrix}$
(2) Stellar depletion		+0.02	$\begin{smallmatrix} +0.08 \\ -0.02 \end{smallmatrix}$
(3a) T_{eff} scale zeropoint		+0.08	± 0.08
(3b) 1-D atmosphere models		+0.00	$\begin{smallmatrix} +0.10 \\ -0.00 \end{smallmatrix}$
(3c) Convective treatment		+0.00	$\begin{smallmatrix} +0.08 \\ -0.00 \end{smallmatrix}$
(3d) NLTE		-0.02	± 0.01
(3e) gf -values		+0.00	± 0.04
(4) Anomalous objects		+0.00	± 0.01
Total		-0.03	$\begin{smallmatrix} +0.19 \\ -0.13 \end{smallmatrix}$
-			-
Inferred:	$A(\text{Li})_p =$	+2.09	$\begin{smallmatrix} +0.19 \\ -0.13 \end{smallmatrix}$

Table Caption:

Table 1: Weighted mean and 95% CL uncertainty of observed Li abundances for a very metal-poor turnoff sample^[3] with $\langle [\text{Fe}/\text{H}] \rangle = -2.8$, and corrections required to deduce the primordial value. (The *weighted* mean differs slightly from the *robust* mean, viz. 2.11^[3].) Five estimates of the logarithmic correction for GCE are listed, based on the previous analysis^[3] (logarithmic fits and observed ${}^6\text{Li}/{}^7\text{Li}$ ratio) and the new work in this paper (linear fits and various GCE models). The model fits are based on the model slopes and the inferred deviation of the primordial value to the weighted mean at $[\text{Fe}/\text{H}] = -2.8$. The various error estimates, which include random and systematic uncertainties, are clearly non-Gaussian, so combining them is an imprecise and subjective process. We take quadratic sums for the positive and negative uncertainties separately, and regard these as estimates of the 95% confidence limits.

Figure captions

Fig. 1 Contributions to the total predicted lithium abundance from the adopted GCE model^[18, 19], compared with low metallicity^[3] and high metallicity^[20] stars. The solid curve is the sum of all components. Additional stellar production mechanisms of ${}^7\text{Li}$ are required for stars with $[\text{Fe}/\text{H}]$ near zero, but are expected to be unimportant for the lowest metallicity objects. The primordial component of ${}^7\text{Li}$ decreases at high metallicity due to astration, but other components increase with metallicity as described in the text. The GCE model^[18, 19] is a one-zone (closed box) model which includes GCR and stellar nucleosynthesis. The latter does not reproduce the observed O-Fe scaling^[15, 16], so we retain the calculated O evolution and force Fe to match $[\text{O}/\text{Fe}] = \omega[\text{Fe}/\text{H}]$, (with $\omega = -0.31$). For GCR production of Li, the model assumes that the cosmic ray flux is proportional to the supernova rate, and that GCR abundances match the ISM. These assumptions fix the linearity of Li-O scaling at low metallicity where $\alpha + \alpha$ dominates. The scale *factor* is set by the GCR particle spectrum and confinement, for which we take a source spectrum $\propto p^{-2}$, and an escape path-length $\Lambda = 100 \text{ g cm}^{-2}$. The model requires three remaining inputs: (1) an adopted primordial ${}^7\text{Li}_p$ abundance, (2) the overall normalization for all GCR production, and (3) the ν -process contribution. As GCR nucleosynthesis also produces beryllium and boron, we use the meteoritic ${}^9\text{Be}$ and ${}^{10}\text{B}$ abundances to establish the overall normalization, which then fixes the GCR contributions to ${}^6\text{Li}$ and ${}^7\text{Li}$. With these normalizations, the modeled evolution of Be and B fits available Population II observations^[18, 19].

Fig. 2 Likelihood distributions for four values of primordial ${}^7\text{Li}/\text{H}$ ($10^{10} \times {}^7\text{Li}/\text{H} = 1.9$ (*dashed*), 1.6 (*dotted*), 1.23 (*solid*), and 0.9 (*dash-dotted*)), and for ${}^4\text{He}$ (*shaded*) for which we adopt $Y_p = 0.238 \pm 0.002 \pm 0.005$ (random and systematic uncertainties)^[17]. For ${}^7\text{Li}/\text{H} = 1.6 \times 10^{-10}$ ($A(\text{Li}) = 2.20$), there are two likely values of $\eta_{10} \equiv 10^{10}\eta = 1.9$ and 3.6, because the predictions are not monotonic in ${}^7\text{Li}$. For ${}^7\text{Li}/\text{H} \lesssim 1.1 \times 10^{-10}$ ($A(\text{Li}) \lesssim 2.04$), the Li abundance is at or below the BBN predicted value, so there is only one peak, at $\eta_{10} \simeq 2.6$; uncertainties in the prediction and observation prevent the likelihood function from vanishing. The peaks of the combined distribution (the product of $L_{4\text{He}}(\eta)$ and $L_{7\text{Li}}(\eta)$; not shown) are at roughly the same value of η as in the individual $L_{7\text{Li}}(\eta)$ distributions.

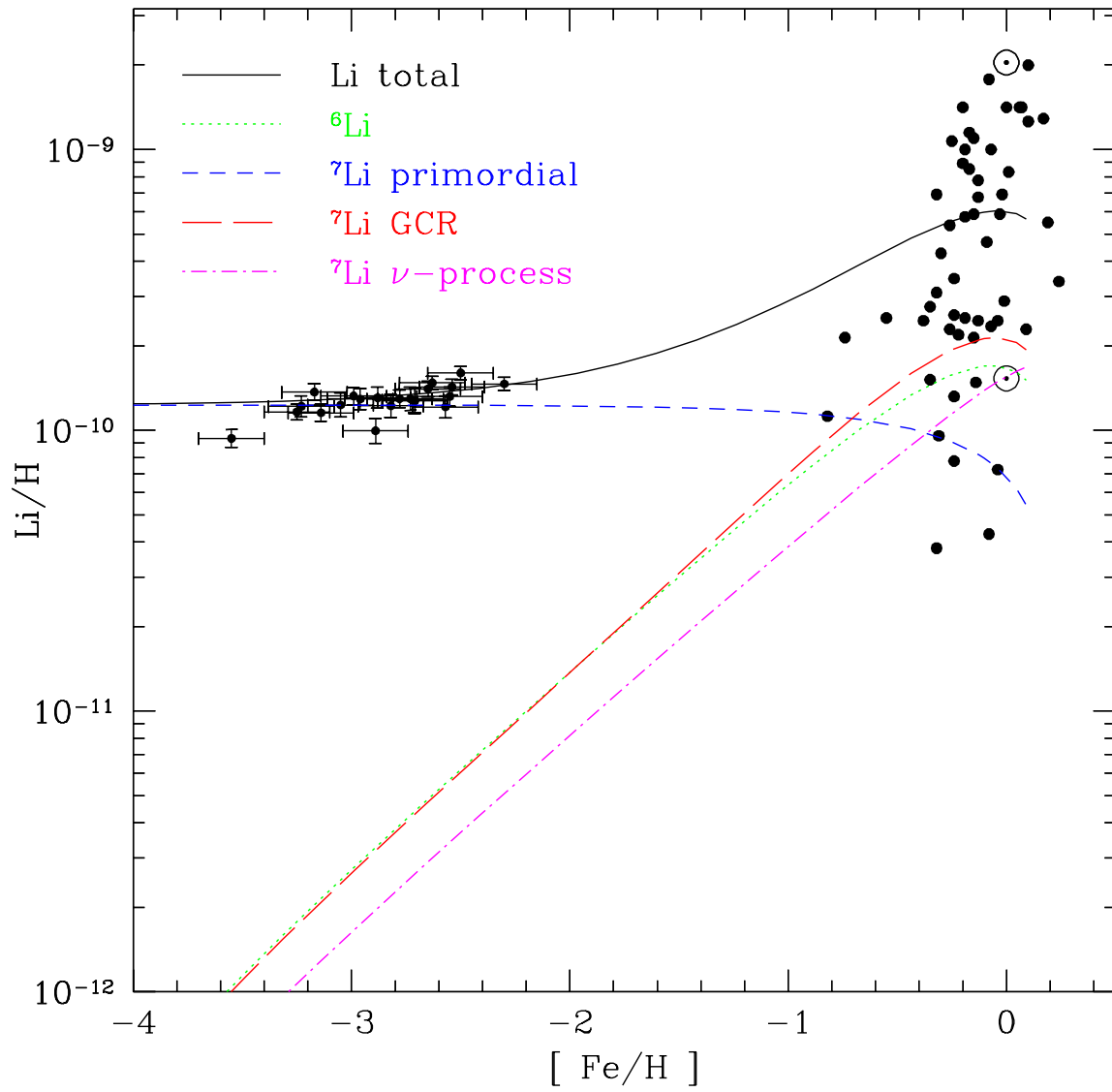


Figure 1

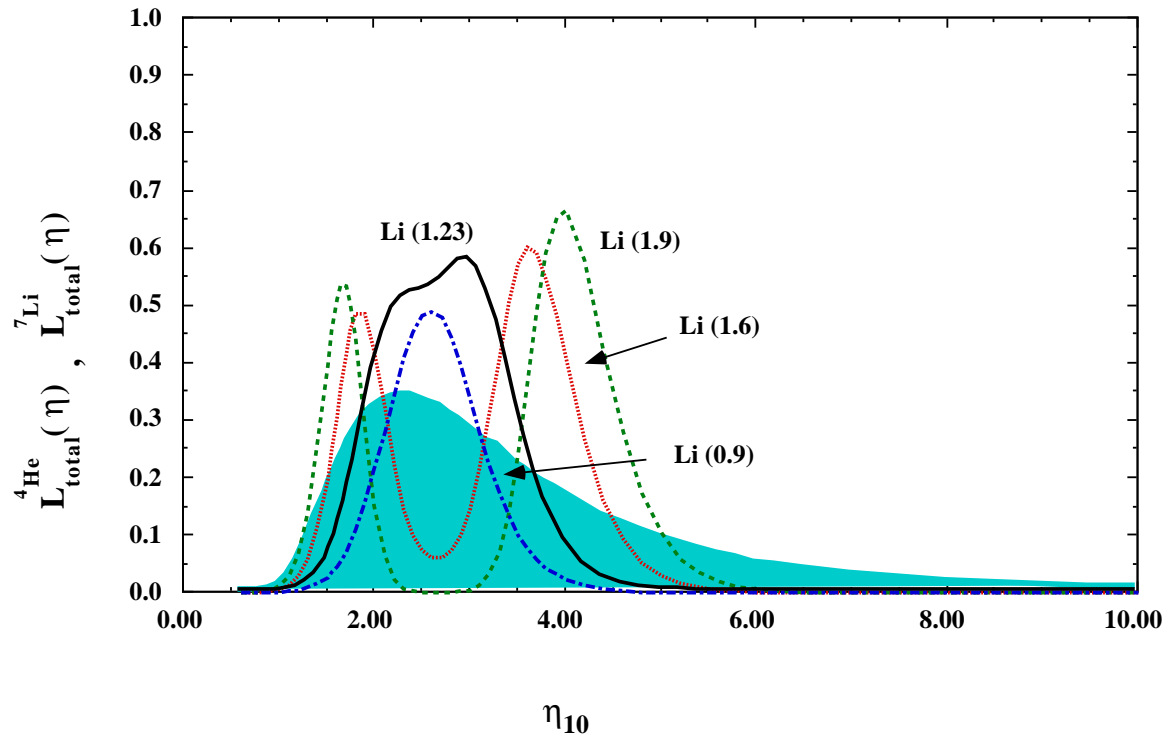


Figure 2